

Partial Oxidation of Methane to Formaldehyde: A Theoretic-Experimental Approach to Process Design and Catalyst Development

Francesco Arena,^{*,1} Francesco Frusteri,[†] and Adolfo Parmaliana^{*}

^{*}Dipartimento di Chimica Industriale e Ingegneria dei Materiali, Università degli Studi di Messina, Salita Sperone 31, I-98166 S. Agata (Messina), Italy; and [†]Istituto CNR-ITAE, Salita S. Lucia 39, I-98126 S. Lucia (Messina), Italy

Received July 3, 2001; revised January 15, 2002; accepted January 15, 2002

The catalytic behaviour and steady-state redox properties of the *precipitated* silica catalyst in methane to formaldehyde partial oxidation (MPO) are addressed and basic relationships between the activity–selectivity pattern and operating conditions of the MPO process are outlined. A set of model equations, accounting for the influence of any experimental parameter (i.e., T , P , $P_{\text{CH}_4}/P_{\text{O}_2}$ ratio, τ) on the steady-state conditions of the catalyst surface and activity–selectivity pattern, constitutes a theoretical background for catalyst optimization and engineering of the MPO reaction. © 2002 Elsevier Science (USA)

Key Words: methane partial oxidation; formaldehyde; silica catalyst; active sites; kinetic modelling; catalyst development; process design.

INTRODUCTION

The large number of research papers focused during the last two decades on the catalytic partial oxidation of methane to formaldehyde (MPO) allowed the peculiar functionality of the silica surface towards HCHO formation to be highlighted (1–4). The preparation method affects the catalytic performance of commercial silica samples (1, 2, 5, 6) according to the activity scale

$$\text{precipitation} > \text{sol-gel} > \text{pyrolysis},$$

as it determines a different density of “strained siloxane bridges” previously claimed to be the active sites in MPO (1, 6). Yet, recent studies on the origin of the catalytic functionality of silicas (7, 8) really pointed to *constitutional* Fe^{3+} ions, incorporated into the matrix during preparation, as the active component enabling the occurrence of redox cycles under MPO conditions (7–9). In particular, we found that isolated Fe^{3+} ions on silicas are responsible for the main reaction path leading to HCHO formation, whereas aggregated Fe^{3+} species mostly yield CO_x (7–9). Actually,

due to a relatively high level (300–400 ppm) of iron impurities (7, 8), the *bare precipitated* SiO_2 Si 4–5P (Akzo product) features the best activity–selectivity pattern and HCHO productivity (STY_{HCHO}) in the range 650–750°C (5, 7–11). That is, by adopting a “continuous flow recirculation” reactor configuration, CH_4 conversion of 35–60% coupled to HCHO selectivity values of 30–56% were attained in the range 650–700°C (10). This promising catalytic performance of the “precipitated” silica catalyst prompted us to investigate in some detail the kinetics and mechanism of the MPO reaction (12, 13). Namely, since redox properties play a crucial role in the catalytic pattern of oxide systems in oxidation reactions (14, 15), we performed a thorough investigation into the steady-state of the catalyst surface by reaction temperature oxygen chemisorption (RTOC), which allowed the kinetics and mechanism of the MPO reaction on the precipitated silica to be highlighted (12, 13). Indeed, a formal Langmuir–Hinshelwood kinetic model, accounting for the competitive activation of both CH_4 and O_2 molecules by a *push–pull* or *concerted* reaction pathway, has been proposed (12–14). Further, on the basis of activation energy values of the redox steps, we stressed that methane activation ($E_{\text{red}} = 112 \text{ kJ} \cdot \text{mol}^{-1}$) is the rate determining step of the MPO on silica catalyst, whilst the oxygen replenishment process ($E_{\text{ox}} \approx 20 \text{ kJ} \cdot \text{mol}^{-1}$) is practically a *nonactivated* reaction step (12, 13). Though such a formal kinetic model allowed successfully prediction of both reaction kinetics and steady-state conditions of the catalytic surface under a wide range of experimental conditions (12, 13), basic relationships accounting for the activity–selectivity pattern and HCHO productivity of a silica-based catalyst, in a perspective of engineering the MPO reaction (9), were not explicitly outlined.

Therefore, this paper aims to provide a thorough description of the activity–selectivity pattern of silica-based catalysts in MPO as a function of operating conditions and physicochemical properties of the catalyst, representing thus a basic tool for future catalyst development and engineering of the MPO process.

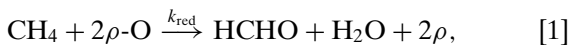
¹ To whom correspondence should be addressed. Fax: +39 090 391518. E-mail: Francesco.Arena@unime.it.

METHODS

The commercial precipitated silica sample (Si 4-5P Grade, Akzo product; SA_{BET} , 380 m²·g⁻¹) was used as catalyst. Activity data at 650°C were obtained using a quartz tube linear reactor (inner diameter, 4 mm) operating either in batch or continuous flow mode, according to the procedures elsewhere described (7–13). The tests were performed using a catalyst sample of 0.050–0.200 g (16–25 mesh) and the reaction mixture He/N₂/CH₄/O₂ in the molar ratio 6/1/2/1 flowing at rates ranging between 100 and 1000 stp cm³·min⁻¹, which accounts for a contact time between 0.008 and 0.08 s. All the gaseous products were analysed online by a HP 5890A gas chromatograph, while HCHO was cumulatively determined at the end of each run by gas chromatography analysis of the condensed (–2°C) reaction products (i.e., HCHO in water) (12, 13).

RESULTS AND DISCUSSION

By evaluating the influence of the $P_{\text{CH}_4}/P_{\text{O}_2}$ ratio on the density of reduced sites (ρ) of the silica surface at 650°C under steady-state conditions by RTOC measurements (12, 13), we previously concluded that the MPO on silica catalysts proceeds via a *two-site-dissociative* activation mechanism of CH₄ and O₂ molecules, pointing to the occurrence of the irreversible surface reactions



where ρ and $\rho\text{-O}$ represent reduced and oxidised forms of the active sites, while k_{red} and k_{ox} are the kinetic constants of the related surface reactions (12, 13). Actually, the occurrence of the above redox cycle leads to the stabilisation of the MPO catalyst in a partially reduced state, enabling the surface uptake of gas-phase O₂ under steady-state conditions (12–15). Taking into account the relationships

$$[\rho] + [\rho\text{-O}] = [\rho_0], \quad [3a]$$

$$[\rho] = [\rho_0] \cdot \theta_{\text{red}}, \quad [3b]$$

$$[\rho\text{-O}] = [\rho_0] \cdot (1 - \theta_{\text{red}}), \quad [3c]$$

with θ_{red} the fractional density of reduced sites (e.g., $[\rho]/[\rho_0]$), at the steady state, since the diffusion rate of bulk O²⁻ ions across the SiO₂ lattice under MPO conditions is negligible (1, 3, 10–13, 16, 17), the mass balance of active sites allows the following equation to be written:

$$k_{\text{ox}} \cdot P_{\text{O}_2} \cdot \rho_0^2 \cdot \theta_{\text{red}}^2 = k_{\text{red}} \cdot P_{\text{CH}_4} \cdot \rho_0^2 \cdot (1 - \theta_{\text{red}})^2. \quad [4]$$

Then, the fractional density of reduced sites (θ_{red}) is given

by the formula

$$\theta_{\text{red}} = \frac{\sqrt{\frac{k_{\text{red}}}{k_{\text{ox}}}} \cdot \left(\frac{P_{\text{CH}_4}}{P_{\text{O}_2}}\right)^{0.5}}{1 + \sqrt{\frac{k_{\text{red}}}{k_{\text{ox}}}} \cdot \left(\frac{P_{\text{CH}_4}}{P_{\text{O}_2}}\right)^{0.5}}, \quad [5]$$

which signals a square-root dependence of the surface reduction degree (θ_{red}) on the $P_{\text{CH}_4}/P_{\text{O}_2}$ ratio (12, 13). Further, since reactions [1] and [2] are irreversible, the rate of methane conversion (rate_{CH₄}) at the steady state must equal that of reaction steps [1] and [2]:

$$\text{rate}_{\text{CH}_4} = k_{\text{ox}} \cdot P_{\text{O}_2} \cdot \rho_0^2 \cdot \theta_{\text{red}}^2 = k_{\text{red}} \cdot P_{\text{CH}_4} \cdot \rho_0^2 \cdot (1 - \theta_{\text{red}})^2. \quad [6]$$

Substituting the θ_{red} value obtained by Eq. [5], the following basic rate equation for the MPO reaction is obtained (12, 13):

$$\text{rate}_{\text{CH}_4} = \rho_0^2 \cdot \frac{k_{\text{red}} \cdot P_{\text{CH}_4}}{\left(1 + \sqrt{\frac{k_{\text{red}} \cdot P_{\text{CH}_4}}{k_{\text{ox}} \cdot P_{\text{O}_2}}}\right)^2}. \quad [7]$$

Denoting methane conversion as the ratio between reaction rate (rate_{CH₄}) and feeding rate (F_{CH_4}),

$$X_{\text{CH}_4} = \frac{k_{\text{red}} \cdot P_{\text{CH}_4} \cdot \rho_0^2 \cdot (1 - \theta_{\text{red}})^2}{F_{\text{CH}_4}}, \quad [8]$$

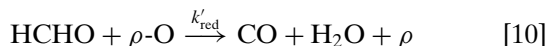
and considering that $P_{\text{CH}_4} = P_{\text{tot}} \cdot X_{\text{CH}_4}$ and $F_{\text{CH}_4} = F_{\text{tot}} \cdot X_{\text{CH}_4}$, Eq. [8] becomes

$$X_{\text{CH}_4} = \frac{P_{\text{tot}}}{F_{\text{tot}}} \cdot k_{\text{red}} \cdot \rho_0^2 \cdot (1 - \theta_{\text{red}})^2, \quad [9]$$

provided that $X_{\text{CH}_4} \leq P_{\text{O}_2, \text{in}}/P_{\text{CH}_4, \text{in}}$.

This relationship implies that at a given temperature T , methane conversion (X_{CH_4}) depends ultimately on the process conditions (e.g., $P_{\text{tot}}/F_{\text{tot}}$), with k_{red} and θ_{red} being related to the nature of the oxide catalyst and redox potential of the reaction mixture (12–15).

However, the catalytic nature of the consecutive oxidation of HCHO to CO and CO₂ (1, 2, 10–13, 16, 17) implies that also the product distribution should depend on the concentration of active sites (12–14, 18, 19). In fact, disregarding the further oxidation of CO to CO₂, which on silica catalysts proceeds slowly (1, 5, 12, 13, 15), the rate of the consecutive oxidation of HCHO to CO according to the stoichiometry



can be expressed as

$$\text{rate}_{\text{CO}} = k'_{\text{red}} \cdot P_{\text{HCHO}} \cdot \rho_0 \cdot (1 - \theta_{\text{red}}), \quad [11]$$

where k'_{red} is the kinetic constant of the surface reaction between HCHO and the oxidised active sites ($\rho\text{-O}$).

Then, the selectivity to HCHO (S_{HCHO}) can be denoted as the ratio between the rate of HCHO formation (i.e., $\text{rate}_{\text{CH}_4} - \text{rate}_{\text{CO}}$) and the overall rate of CH_4 conversion,

$$S_{\text{HCHO}} = \frac{[k_{\text{red}} \cdot P_{\text{CH}_4} \cdot \rho_0^2 \cdot (1 - \theta_{\text{red}})^2 - k'_{\text{red}} \cdot P_{\text{HCHO}} \cdot \rho_0 \cdot (1 - \theta_{\text{red}})]}{k_{\text{red}} \cdot P_{\text{CH}_4} \cdot \rho_0^2 \cdot (1 - \theta_{\text{red}})^2}, \quad [12]$$

which can be simplified into the following relationship:

$$S_{\text{HCHO}} = 1 - \frac{k'_{\text{red}} \cdot P_{\text{HCHO}}}{k_{\text{red}} \cdot P_{\text{CH}_4} \cdot \rho_0 \cdot (1 - \theta_{\text{red}})}. \quad [13]$$

In general terms, P_{HCHO} can be expressed as:

$$P_{\text{HCHO}} = \bar{X}_{\text{CH}_4} \cdot P_{\text{CH}_4}, \quad [14]$$

where for \bar{X}_{CH_4} , on the assumption of a differential conversion level ($<1\%$), the arithmetic average value of X_{CH_4} (e.g., $X_{\text{CH}_4}/2$) can be taken. Then, combining Eqs. [9], [13], and [14], the final expression for derivative changes in HCHO selectivity becomes

$$S_{\text{HCHO}} = 1 - \left[\frac{k'_{\text{red}}}{2} \cdot \frac{P_{\text{tot}}}{F_{\text{tot}}} \cdot \rho_0 \cdot (1 - \theta_{\text{red}}) \right], \quad [15]$$

while that for the CO selectivity (S_{CO}) results in

$$S_{\text{CO}} = \left[\frac{k'_{\text{red}}}{2} \cdot \frac{P_{\text{tot}}}{F_{\text{tot}}} \cdot \rho_0 \cdot (1 - \theta_{\text{red}}) \right]. \quad [16]$$

These last two equations indicate that also the product distribution in the MPO reaction is definitively affected by the process conditions, as k'_{red} is still related to the nature of the catalyst (12, 13).

From a practical point of view, the above relationships imply that the activity–selectivity pattern of silica catalysts in MPO can be predicted and tuned by a suitable design of the process conditions. In addition, Eqs. [9], [15], and [16] provide a basic explanation to the experimental dependence of conversion and selectivity both on contact time (τ) and steady-state conditions of the catalyst surface (9–19). Indeed, a rise in contact time (i.e., $\tau \propto F_{\text{tot}}^{-1}$) implies an increase in both X_{CH_4} (Eq. [9]) and S_{CO} (Eq. [16]) and a parallel decrease (Eq. [15]) in S_{HCHO} . Moreover, it is outlined that a deeper reduction of the catalytic surface enables higher S_{HCHO} values ($S_{\text{HCHO}} \rightarrow 1$ per $\theta_{\text{red}} \rightarrow 1$), according to the general pattern of catalytic selective oxidation reactions (12–14, 18, 19).

At least, combining Eqs. [6] and [15], the following mathematical relationship for HCHO productivity (STY_{HCHO}) is found:

$$\text{STY}_{\text{HCHO}} (\text{g} \cdot \text{kg}_{\text{cat}}^{-1} \cdot \text{h}^{-1}) = \alpha \cdot k_{\text{red}} \cdot P_{\text{CH}_4} \cdot \rho_0^2 \cdot (1 - \theta_{\text{red}})^2 \cdot \left[1 - \frac{k'_{\text{red}}}{2} \cdot \frac{P_{\text{tot}}}{F_{\text{tot}}} \cdot \rho_0 \cdot (1 - \theta_{\text{red}}) \right], \quad [17]$$

where $\alpha = 10.8 \times 10^6 \text{ g} \cdot \text{kg}_{\text{cat}}^{-1} \cdot \text{h}^{-1} \cdot (\text{mol}^{-1} \cdot \text{g}_{\text{cat}} \cdot \text{S})$.

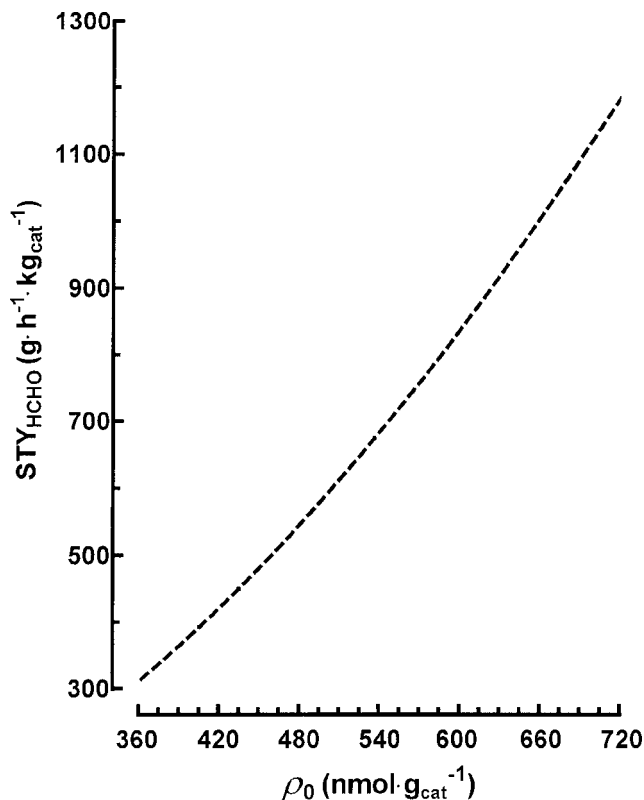


FIG. 1. Partial oxidation of methane to formaldehyde. HCHO productivity (STY_{HCHO}) vs total concentration of active sites (ρ_0) at 650°C ($P_{\text{CH}_4, \text{in}}/P_{\text{O}_2, \text{in}} = 2$) as calculated using Eq. [17] on the basis of k_{red} , θ_{red} , and k'_{red} values of the precipitated SiO_2 Si 4–5P catalyst (12, 13).

Since the reaction rate ($\text{rate}_{\text{CH}_4}$) rises according to a second-order relationship with respect to the concentration of active sites (ρ_0), while the HCHO selectivity decreases with ρ_0 by a third-order dependence, productivity will suddenly increase with ρ_0 , as shown in Fig. 1, where, assuming k'_{red} (vide infra), k_{red} ($9.0 \times 10^7 \text{ g} \cdot \text{mol}^{-1} \cdot \text{s}^{-1} \cdot \text{atm}^{-1}$), k_{ox} ($1.9 \times 10^{10} \text{ g} \cdot \text{mol}^{-1} \cdot \text{s}^{-1} \cdot \text{atm}^{-1}$), and θ_{red} (0.08) values previously determined at 650°C for $P_{\text{CH}_4}/P_{\text{O}_2} = 2$ on the studied catalyst (12, 13), the trend of the STY_{HCHO} vs ρ_0 is outlined. Notably, such a finding signals that the STY_{HCHO} of silica-based catalysts would be timely, promoted by a preparation route enabling higher concentrations of MPO active sites (7–9, 20).

A complete description of the activity–selectivity pattern of the precipitated silica catalyst to attain a proper design of the MPO process still lacks basic relationships relating S_{HCHO} to contact time (τ) and methane conversion (X_{CH_4}). In this respect, it has been previously shown that S_{HCHO} depends on the $P_{\text{tot}}/F_{\text{tot}}$ ratio and on P_{HCHO} , whose value is actually a function of X_{CH_4} . Thus, an integral expression for S_{HCHO} can be obtained assuming that the catalytic bed behaves like a semibatch reactor with continuous feeding of the reaction mixture. In such a case, the same model equation accounting for the kinetics of homogeneous consecutive reactions ($A \xrightarrow{K_1} B \xrightarrow{K_2} C$) in a batch reactor

system,

$$S_B = \frac{K_1}{(K_2 - K_1)} \cdot \frac{(e^{-K_1 \cdot t} - e^{-K_2 \cdot t})}{(1 - e^{-K_1 \cdot t})}, \quad [18]$$

should match the influence of contact time on S_{HCHO} , provided that A , B , and C stand for CH₄, HCHO, and CO, respectively, and that reaction time (t) is replaced by the $P_{\text{tot}}/F_{\text{tot}}$ (atm · mol⁻¹ · s · g_{cat}) parameter. Accordingly, with the kinetic constants K_1 and K_2 in such a case being equal to $[(k'_{\text{red}}) \cdot (\rho_0)^2 \cdot (1 - \theta_{\text{red}})^2]$ and $[(k'_{\text{red}}) \cdot (\rho_0) \cdot (1 - \theta_{\text{red}})]$, respectively, the following expression for S_{HCHO} vs $P_{\text{tot}}/F_{\text{tot}}$ is found:

$$S_{\text{HCHO}} = \frac{k_{\text{red}} \cdot \rho_0 \cdot (1 - \theta_{\text{red}})}{[k'_{\text{red}} - k_{\text{red}} \cdot \rho_0 \cdot (1 - \theta_{\text{red}})]} \cdot \frac{\left(e^{-k_{\text{red}} \cdot \rho_0^2 \cdot (1 - \theta_{\text{red}})^2 \cdot \left(\frac{P_{\text{tot}}}{F_{\text{tot}}} \right)} - e^{-k'_{\text{red}} \cdot \rho_0 \cdot (1 - \theta_{\text{red}}) \cdot \left(\frac{P_{\text{tot}}}{F_{\text{tot}}} \right)} \right)}{\left(1 - e^{-k_{\text{red}} \cdot \rho_0^2 \cdot (1 - \theta_{\text{red}})^2 \cdot \left(\frac{P_{\text{tot}}}{F_{\text{tot}}} \right)} \right)}. \quad [19]$$

Further, deriving the value of the $P_{\text{tot}}/F_{\text{tot}}$ parameter from Eq. [9],

$$\frac{P_{\text{tot}}}{F_{\text{tot}}} = \frac{X_{\text{CH}_4}}{k_{\text{red}} \cdot \rho_0^2 \cdot (1 - \theta_{\text{red}})^2}, \quad [20]$$

results show that HCHO selectivity is also related to CH₄ conversion by the following equation:

$$S_{\text{HCHO}} = \frac{k_{\text{red}} \cdot \rho_0 \cdot (1 - \theta_{\text{red}})}{[k'_{\text{red}} - k_{\text{red}} \cdot \rho_0 \cdot (1 - \theta_{\text{red}})]} \cdot \frac{\left(e^{-X_{\text{CH}_4}} - e^{-k'_{\text{red}} \cdot \frac{X_{\text{CH}_4}}{k_{\text{red}} \cdot \rho_0 \cdot (1 - \theta_{\text{red}})}} \right)}{(1 - e^{-X_{\text{CH}_4}})}. \quad [21]$$

Then, the trends of CH₄ conversion and HCHO selectivity vs the $P_{\text{tot}}/F_{\text{tot}}$ ratio and that of S_{HCHO} vs X_{CH_4} , as calculated using Eqs. [9], [19], and [21], are compared in Figs. 2A and 2B, respectively, with experimental X_{CH_4} and S_{HCHO} data at 650°C and at different contact times. The good agreement between experimental and calculated data is the most relevant proof of the reliability of the above model equations in predicting the behaviour of MPO catalysts, while the nonlinear regression analysis of the above curves provides a k'_{red} value equal to $2.55 \times 10^3 \text{ atm}^{-1} \cdot \text{s}^{-1}$. Moreover, the empirical inverse relationship between S_{HCHO} and CH₄ conversion, generally valid for MPO reactions (1–5, 10, 11, 18–20), is highlighted on a scientific basis.

It appears that the above relationships provide a comprehensive mathematical description of the activity–selectivity pattern of MPO catalysts on the basis of kinetic parameters related to both redox properties of the silica catalyst and

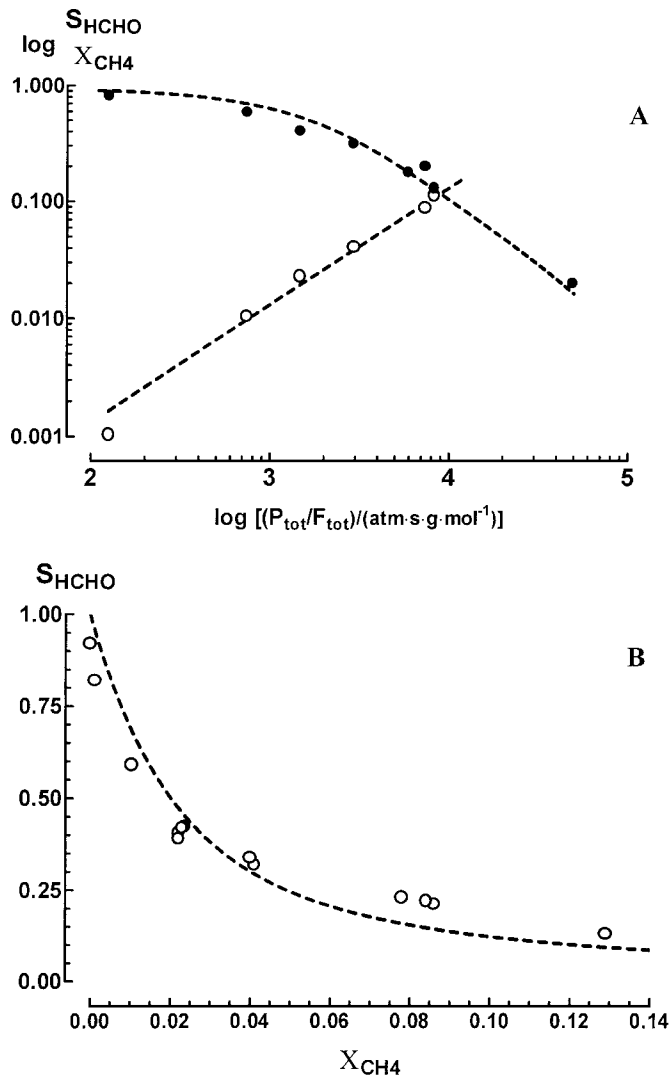


FIG. 2. Partial oxidation of methane to formaldehyde. (A) Theoretical curves (Eqs. [9] and [19]) and experimental HCHO selectivity (S_{HCHO} , ●) and CH₄ conversion (X_{CH_4} , ○) data of the precipitated SiO₂ Si 4–5P catalyst at 650°C vs contact time ($P_{\text{tot}}/F_{\text{tot}}$ ratio). (B) Theoretical curve (Eq. [21]) and experimental S_{HCHO} vs X_{CH_4} data of the precipitated SiO₂ Si 4–5P catalyst at 650°C.

operating conditions. That is, the above set of equations constitutes a scientific background for catalyst development and engineering of the MPO reaction, representing a basic contribution to catalysis and process design of selective oxidation reactions.

CONCLUSIONS

The activity–selectivity pattern and surface properties at steady state of precipitated silica catalysts in MPO have been studied and thoroughly related to the physicochemical properties of the solid and operating conditions (T , P , $P_{\text{CH}_4}/P_{\text{O}_2}$, τ).

In particular, the main results of this work can be summarised as follows:

- The density of reduced sites of the catalyst under steady-state conditions depends on the square root of the $P_{\text{CH}_4}/P_{\text{O}_2}$ ratio.
- Basic equations account for the dependence of CH_4 conversion and HCHO selectivity on contact time; the origin of the inverse relationship between HCHO selectivity and CH_4 conversion is also highlighted on a formal scientific basis.
- The HCHO productivity (STY) of silica-based catalysts rises according to a *quasi* second-order dependence on the concentration of active sites.
- A set of model equations allows a full tuning of the MPO reaction, representing thus a basic tool for further catalyst optimisation and process design.

ACKNOWLEDGMENT

This work has been realized in the framework of a research contract between SÜD CHEMIE Ag (München, Germany) and University of Messina (Messina, Italy).

REFERENCES

1. Sun, Q., Herman, R. G., and Klier, K., *Catal. Lett.* **16**, 251 (1992).

2. Parmaliana, A., Frusteri, F., Mezzapica, A., Miceli, D., Scurrrell, M. S., and Giordano, N., *J. Catal.* **143**, 262 (1993).
3. Koranne, M. M., Goodwin, J. G., and Marcelin, G., *J. Catal.* **148**, 378 (1994).
4. Parmaliana, A., and Arena, F., *J. Catal.* **167**, 57 (1997).
5. Arena, F., Frusteri, F., Parmaliana, A., and Giordano, N., *Appl. Catal. A* **125**, 39 (1995).
6. Vikulov, K., Martra, G., Coluccia, S., Miceli, D., Arena, F., Parmaliana, A., and Paukshtis, E., *Catal. Lett.* **37**, 235 (1996).
7. Arena, F., Frusteri, F., Fierro, J. L. G., and Parmaliana, A., *Stud. Surf. Sci. Catal.* **136**, 531 (2001).
8. Parmaliana, A., Arena, F., Frusteri, F., Martinez-Ariaz, A., Lopez-Granados, M., and Fierro, J. L. G., *Appl. Catal. A*, in press.
9. Parmaliana, A., Arena, F., Frusteri, F., and Mezzapica, A., German Patent 100,544,576 (2000).
10. Parmaliana, A., Arena, F., Frusteri, F., and Mezzapica, A., *Stud. Surf. Sci. Catal.* **110**, 665 (1998).
11. Parmaliana, A., Sokolovskii, V., Miceli, D., Arena, F., and Giordano, N., *J. Catal.* **148**, 514 (1994).
12. Arena, F., Frusteri, F., and Parmaliana, A., *Appl. Catal. A* **197**, 239 (2000).
13. Arena, F., Frusteri, F., and Parmaliana, A., *AIChE J.* **46**, 2285 (2000).
14. Bielański, A., and Haber, J., "Oxygen in Catalysis." Dekker, New York, 1991.
15. Sokolovskii, V., *Catal. Rev.-Sci. Eng.* **32**, 1 (1990).
16. Arena, F., Giordano, N., and Parmaliana, A., *J. Catal.* **167**, 66 (1997).
17. Amiridis, M. D., Rekoske, J. E., Dumesic, J. A., Rudd, D. F., Spencer, N. D., and Pereira, C. J., *AIChE J.* **37**, 87 (1991).
18. Kasztelan, S., *Ind. Eng. Chem. Res.* **31**, 2497 (1992).
19. Kung, H. H., *J. Catal.* **134**, 691 (1992).
20. Arena, F., Frusteri, F., Torre, M., Venuto, A., and Parmaliana, A., *Catal. Lett.*, in press.